Signal Transduction:

Actin Dynamics Regulated by the Balance of Neuronal Wiskott-Aldrich Syndrome Protein (N-WASP) and Cofilin Activities Determines the Biphasic Response of Glucose-induced Insulin Secretion

Eita Uenishi, Tadao Shibasaki, Harumi Takahashi, Chihiro Seki, Hitomi Hamaguchi, Takao Yasuda, Masao Tatebe, Yutaka Oiso, Tadaomi Takenawa and Susumu Seino

J. Biol. Chem. 2013, 288:25851-25864.
doi: 10.1074/jbc.M113.464420 originally published online July 18, 2013

THE JOURNAL OF BIOLOGICAL CHEMISTRY VOL. 288, NO. 36, pp. 25851–25864, September 6, 2013

Actin Dynamics Regulated by the Balance of Neuronal Wiskott-Aldrich Syndrome Protein (N-WASP) and Cofilin Activities Determines the Biphasic Response of Glucose-induced Insulin Secretion*

Received for publication, February 24, 2013, and in revised form, July 8, 2013 Published, JBC Papers in Press, July 18, 2013, DOI 10.1074/jbc.M113.464420

Eita Uenishi[‡§1], Tadao Shibasaki[‡1], Harumi Takahashi[‡], Chihiro Seki[‡], Hitomi Hamaguchi[‡], Takao Yasuda[‡], Masao Tatebe[‡], Yutaka Oiso[§], Tadaomi Takenawa[¶‖], and Susumu Seino[‡‖‡‡2]**

*From the [‡]Division of Cellular and Molecular Medicine, **Division of Molecular and Metabolic Medicine, [¶]Division of Lipid Biochemistry, and the [‖]Integrated Center for Mass Spectrometry, Kobe University Graduate School of Medicine, Kobe 650-0017, the [§]Department of Endocrinology and Diabetes, Nagoya University Graduate School of Medicine, Nagoya 466-8550, and the [‡‡]Core Research for Evolutional Science and Technology (CREST), Japan Science and Technology Corp., Kawaguchi, Saitama 332-0012, Japan*

Background: Actin dynamics is involved in insulin secretion, but the mechanism is unknown.
Results: The G-actin predominant or F-actin remodeling state in pancreatic β-cells, which is regulated by the balance of N-WASP and cofilin activities, determines the biphasic glucose-induced insulin secretion (GIIS).
Conclusion: Actin dynamics regulated by N-WASP and cofilin underlie the biphasic GIIS.
Significance: The regulation of actin dynamics in β-cells and its role in GIIS are clarified.

Actin dynamics in pancreatic β-cells is involved in insulin secretion. However, the molecular mechanisms of the regulation of actin dynamics by intracellular signals in pancreatic β-cells and its role in phasic insulin secretion are largely unknown. In this study, we elucidate the regulation of actin dynamics by neuronal Wiskott-Aldrich syndrome protein (N-WASP) and cofilin in pancreatic β-cells and demonstrate its role in glucose-induced insulin secretion (GIIS). N-WASP, which promotes actin polymerization through activation of the actin nucleation factor Arp2/3 complex, was found to be activated by glucose stimulation in insulin-secreting clonal pancreatic β-cells (MIN6-K8 β-cells). Introduction of a dominant-negative mutant of N-WASP, which lacks G-actin and Arp2/3 complex-binding region VCA, into MIN6-K8 β-cells or knockdown of N-WASP suppressed GIIS, especially the second phase. We also found that cofilin, which severs F-actin in its dephosphorylated (active) form, is converted to the phosphorylated (inactive) form by glucose stimulation in MIN6-K8 β-cells, thereby promoting F-actin remodeling. In addition, the dominant-negative mutant of cofilin, which inhibits activation of endogenous cofilin, or knockdown of cofilin reduced the second phase of GIIS. However, the first phase of GIIS occurs in the G-actin predominant state, in which cofilin activity predominates over N-WASP activity. Thus, actin dynamics regulated by the balance of N-WASP and cofilin activities determines the biphasic response of GIIS.

Insulin secretion from pancreatic β-cells plays the central role in maintaining glucose homeostasis; dysfunction of insulin secretion is the major contributor to the pathogenesis and pathophysiology of type 2 diabetes mellitus (1–3). Insulin secretion is a highly dynamic process regulated by complex mechanisms involving various intracellular signals generated by nutrients and hormonal and neural inputs (4), among which glucose is the most important. Insulin secretion in response to glucose stimulation occurs in a biphasic pattern as follows: an initial component (first phase), which develops rapidly but lasts only a few minutes, followed by a sustained component (second phase) (5–7). Although the molecular mechanism underlying the biphasic kinetics of glucose-induced insulin secretion (GIIS)[3] is poorly understood, it is thought to include interaction of intracellular signals with distinct insulin granule pools (8). It is generally thought that pancreatic β-cells contain at least two pools of insulin secretory granules that differ in release competence as follows: a reserve pool (RP) that accounts for most of the granules, and a readily releasable pool (RRP) that accounts for the other <5% (9, 10). According to the prevailing model of GIIS, the release of insulin granules from RRP comprising predocked granules accounts for the first phase and a subsequent supply of new granules mobilized from RP accounts for the second phase (8). However, we have found that both the first phase and the second phase of GIIS are caused by granules that

* This work was supported by a CREST grant from the Japan Science and Technology Agency, a grant-in-aid for scientific research, and a grant for the Global Centers of Excellence Program "Global Center of Excellence for Education and Research on Signal Transduction Medicine in the Coming Generation" from the Ministry of Education, Culture, Sports, Science and Technology.

[1] Both authors contributed equally to this work.

[2] To whom correspondence should be addressed: Division of Molecular and Metabolic Medicine, Kobe University graduate School of Medicine, Kobe 650-0017, Japan. Tel.: 81-78-304-6061; Fax: 81-78-304-6046; E-mail: seino@med.kobe-u.ac.jp.

[3] The abbreviations used are: GIIS, glucose-induced insulin secretion; Arp2/3, actin-related proteins 2 and 3; N-WASP, neuronal Wiskott-Aldrich syndrome protein; RRP, readily releasable pool; RP, reserve pool; TIRFM, total internal reflection fluorescence microscopy; DN, dominant-negative; AUC, area under the curve.

are newly recruited and immediately fused to the plasma membrane without docking ("*restless newcomer*") (11). We propose that the first phase results from RRP near the plasma membrane and the second phase from RP located a distance away from the plasma membrane (11, 12). It has been suggested that the cortical actin network is also involved in the dynamics of insulin secretion (13, 14). It is well known that impaired dynamics of insulin secretion contributes to the pathogenesis and pathophysiology of diabetes (3).

In many eukaryotic cells, actin forms a complex and dynamic network beneath the plasma membrane (15). The rapid remodeling of this network plays an important role in the regulation of exocytosis in secretory cells such as chromaffin cells and exocrine cells and their derived cell lines (16, 17). An early study showed that F-actin in pancreatic β-cells is organized as a cortical network beneath the plasma membrane (18). The cortical actin network was originally thought to be a physical barrier for insulin granules to reach the plasma membrane (19–21). The role of F-actin in insulin secretion has so far been studied primarily using pharmacological agents. For example, it was shown that F-actin-depolymerizing agents such as cytochalasin B enhance insulin secretion (18). It was also reported that cytochalasin E and *Clostridium botulinum* C2 toxin, which are F-actin-depolymerizing agents, decrease insulin secretion (22). More recently, latrunculin B, which binds to G-actin and leads to F-actin depolymerization, was shown to potentiate GIIS (23). It was also reported that F-actin is not essential in the metabolic amplifying pathway of GIIS, using cytochalasin B, latrunculin B, and jasplakinolide (23). These disparate findings on the role of F-actin in insulin secretion may partly be due to limitation of the pharmacological approach. Various small GTPases, including Rho (24), Cdc42 (13, 25), and Rac (26) and ezrin, radixin, and moesin proteins (27), are known to be involved in F-actin remodeling in GIIS. It has been shown that Cdc42 is activated by glucose stimulation in MIN6 cells (13, 25). Cdc42 has recently been demonstrated to be required for the second phase of GIIS from isolated mouse islets and MIN6 cells (13). Cool-1/β-Pix, one of the guanine nucleotide exchange factors against Cdc42 and Rac1, directly converts Cdc42 to the GTP-bound active form in MIN6 cells in a glucose-dependent manner (28). Cdc42 has a large number of effectors that regulate F-actin remodeling (29). N-WASP links Cdc42 to actin polymerization through the actin-related protein 2/3 (Arp2/3) complex, which promotes actin nucleation (30). Cofilin, which is a downstream signal of Cdc42 and other members of the Rho family, is also an important regulator of actin dynamics (31, 32). Cofilin promotes actin depolymerization by severing F-actin (33, 34). It has been shown that the coordination of N-WASP and cofilin activities in F-actin remodeling is critical for the regulation of invadopodium assembly and maturation in carcinoma cells (35) and migration of endothelial cells (36). However, little is known of the molecular mechanisms of actin dynamics in pancreatic β-cells and its role in phasic insulin secretion.

In this study, we show that interaction of N-WASP activated by Cdc42 and Arp2/3 complex is required for GIIS, especially its second phase. We also show that cofilin, which severs F-actin in its dephosphorylated form (active form), is converted to the phosphorylated form (inactive form) upon glucose stimulation, thereby promoting the F-actin remodeling necessary for the second phase of GIIS. In contrast, the first phase of GIIS is dependent mostly on the G-actin-predominant process. Thus, actin dynamics is regulated by the balance of N-WASP and cofilin activities, and it is critical in determining the biphasic response of GIIS.

EXPERIMENTAL PROCEDURES

Materials—EZ-Detect Cdc42 activation kit containing mouse anti-Cdc42 antibody was purchased from Pierce. Phosphatase inhibitor mixture was from Calbiochem. Protease inhibitor mixture was from Roche Diagnostics. Alexa Fluor488-conjugated donkey anti-rabbit IgG antibody and NucRed Live 647 ReadyProbe reagent were from Invitrogen. Rabbit anti-N-WASP antibody was from Santa Cruz Biotechnology (Santa Cruz, CA). Rabbit anti-LIMK1, anti-PAK1, anti-cofilin, and anti-phospho-cofilin (serine 3) antibodies were from Cell Signaling Technology (Danvers, MA). Anti-phospho-LIMK1 (threonine 508) and anti-phospho-N-WASP (tyrosine 253) antibodies were from ECM Biosciences (Versailles, KY). Rabbit anti-p34-ARC antibody was from Millipore (San Diego). AcGFP1-actin, mCherry, and mOrange cDNAs were from Takara Bio (Shiga, Japan). Nifedipine, IPA3, and PP2 were from Sigma. Y27632 was from Wako Pure Chemical Industries (Osaka, Japan).

Cell Culture—MIN6-K8 β-cells were grown in Dulbecco's modified Eagle's medium (DMEM) containing 10% heat-inactivated fetal bovine serum and maintained in a humidified incubator with 95% air and 5% CO_2 at 37 °C (37).

Site-directed Mutagenesis and Constructions of Adenoviral Vectors—In cofilin, serine at position 3 was substituted with aspartate for a phosphomimetic mutant (cofilin S3D) (38), which is constitutively inactive, using PCR-based methods. Recombinant adenovirus carrying rat wild-type N-WASP (N-WASP WT), dominant-negative mutant of N-WASP (N-WASP DN), which lacks VCA region (39), mCherry-tagged wild-type N-WASP (mCherry-N-WASP WT) or mCherry-tagged dominant-negative N-WASP (mCherry-N-WASP DN), mCherry-*CAAX* (where *AA* indicates aliphatic amino acid), AcGFP1-actin, or cofilin S3D was generated, using ViraPower™ adenoviral expression system (Invitrogen).

Small Hairpin Loop RNA (shRNA)—The shRNA sequences against mouse Cdc42 (GenBank™ accession number MMU37720) and mouse p34-ARC (GenBank™ accession number NM_029711) genes were chosen according to BLOCK-iT RNAi designer of Invitrogen. The target sequences were designed as follows: Cdc42 shRNA top strand, 5′-CACCGGTCTCTCCATCCTCATTTGACGAATCAAATGAGGATGGAGAGACC-3′, and bottom strand, 5′-AAAAGGTCTCTCCATCCTCATTTGATTCGTCAAATGAGGATGGAGAGACC-3; and p34-ARC shRNA top strand, 5′-CACCGCCTATATTCATACACGAATGCGAACATTCGTGTATGAATATAGGC-3′, and bottom strand, 5′-AAAAGCCTATATTCATACACGAATGTTCGCATTCGTGTATGAATATAGGC-3′. shRNA vectors were constructed using the BLOCK-iT adenoviral RNAi expression system (Invitrogen) according to the manufacturer's instructions and subjected to Cdc42 and p34-ARC knockdown experiments.

Small Interfering RNA (siRNA)—For N-WASP and cofilin knockdown experiments, siRNAs (ON-TARGET plus SMART pool and ON-TARGET plus nontargeting pool) were purchased from Dharmacon (Lafayette, CO). MIN6-K8 β-cells were transfected with siRNAs using DharmaFECT2 transfection reagent (Dharmacon) according to the manufacturer's instructions.

Pulldown Assay for Cdc42-GTP—To specifically detect the GTP-bound Cdc42, the EZ-Detect Cdc42 activation kit was used. MIN6-K8 β-cells were incubated for 24 h in DMEM containing 0.1% FBS. Thirty minutes after preincubation in HEPES-balanced Krebs-Ringer bicarbonate (KRB) buffer (119 mM NaCl, 4.74 mM KCl, 2.54 mM $CaCl_2$, 1.19 mM $MgCl_2$, 1.19 mM KH_2PO_4, 25 mM $NaHCO_3$, and 10 mM HEPES, pH 7.4) containing 0.1% BSA with 2.8 mM glucose, the cells were stimulated with HEPES/KRB buffer containing 16.7 mM glucose or 60 mM K^+ for 3 and 15 min. The cell lysates were incubated with 20 μg of GST-PAK1-PBD-agarose for 1 h at 4 °C. The bound proteins were also subjected to SDS-PAGE, followed by Western blot analysis with anti-Cdc42 antibody. The relative abundance of eluted Cdc42 was determined by densitometry.

Coimmunoprecipitation Experiments—Coimmunoprecipitation experiments were performed using ExactaCruz (Santa Cruz Biotechnology) according to the manufacturer's instructions. One hour after preincubation, MIN6-K8 β-cells were treated with HEPES/KRB buffer containing 2.8 or 16.7 mM glucose for 3 and 15 min. The cell lysates were incubated with anti-Cdc42 antibody conjugated with agarose beads. After incubation at 4 °C for 1 h, the beads were washed three times with PBS, and the bound proteins were subjected to SDS-PAGE, followed by Western blot analysis with anti-N-WASP and anti-PAK1 antibodies.

Insulin Secretion Experiments—Mouse pancreatic islets were isolated from 12- to 16-week-old C57BL/6J male mice by collagenase digestion and cultured for 2 days as described previously (40). Insulin released in the incubation buffer and cellular insulin content in mouse islets and MIN6-K8 β-cells were measured by insulin assay kits from Medical Biological Laboratories (Nagoya, Japan) and CIS Bio international (Gif sur Yvette, France), respectively. The amount of insulin secretion was normalized by cellular insulin content.

TIRFM Analysis of Actin Dynamics—Primary cultured β-cells isolated from mouse pancreatic islets were infected with adenovirus carrying AcGFP1-actin together with mCherry, mCherry-N-WASP WT, or mCherry-N-WASP DN for 2 days. After 30 min of preincubation with 2.8 mM glucose, the fluorescence intensity of AcGFP1-actin near the plasma membrane was monitored using TIRFM (IX71, Olympus, Tokyo, Japan) in the cells stimulated with 16.7 mM glucose.

TIRFM Analysis of Insulin Granule Exocytosis—Primary cultured β-cells isolated from mouse pancreatic islets were infected with adenovirus carrying insulin-Venus together with mCherry-N-WASP WT or mCherry-N-WASP DN for 2 days and were subjected to TIRFM analysis as described previously (11). The number of insulin-Venus-containing granules docked to the plasma membrane was measured by G-Count software (G-Angstrom K.K, Miyagi, Japan) as described previously (41).

Immunocytochemical Analysis—MIN6-K8 β-cells were infected with adenovirus carrying mCherry-C*AAX*, which targets to the plasma membrane, and cultured for 2 days. After 30 min of preincubation, MIN6-K8 β-cells were stimulated by 16.7 mM glucose for 3 and 15 min or 60 mM K^+ for 3 min. The cells were fixed in 3.7% formaldehyde and treated with 0.2% Triton X-100 and 10% normal donkey serum. They were incubated with rabbit anti-N-WASP antibody at 4 °C overnight, followed by Alexa Fluor488-labeled donkey anti-rabbit IgG antibody at room temperature for 30 min. After immunostaining, the cells were counterstained with NucRed Live 647 ReadyProbe reagent at room temperature for 30 min. The stained cells were observed by confocal laser scanning microscopy (FV1000, Olympus).

mRNA Expression—Total RNA from MIN6-K8 β-cells was isolated using the RNeasy kit (Qiagen, Hilden, Germany). For reverse transcription, ReverTra Ace-α-kit (Toyobo, Osaka, Japan) was used. Real time PCR was performed using TaqMan probe with a model 7000 real time thermal cycler from Applied Biosystems (Foster City, CA). Measurement of the expression levels of hypoxanthine phosphoribosyltransferase was used as internal control.

Perifusion Experiments—Perifusion experiments on insulin secretion of MIN6-K8 β-cells were performed as described previously (42). Briefly, the cells were seeded on coverslips. The following day, the cells were infected with adenovirus carrying mCherry, mCherry-N-WASP WT, mCherry-N-WASP DN, cofilin WT, or cofilin S3D or transfected with ON-TARGET plus nontargeting pool siRNA (control) or ON-TARGET plus SMART pool siRNAs against N-WASP and cofilin. After 2 days, the cells were perifused in HEPES/KRB buffer containing 2.8 mM glucose for 5 min, and the perfusate was then switched to HEPES/KRB buffer containing 16.7 mM glucose. Each fraction was collected at 1-min intervals, and the released insulin was measured by insulin assay kit (CIS Bio international). The amount of secreted insulin was normalized by cellular insulin content.

Statistical Analysis—Data are presented as mean ± S.E. Statistical analysis was performed by unpaired, two-tailed Student's *t* test or one- or two-way analysis of variance with Tukey's post hoc test. Differences between groups were considered statistically significant when $p < 0.05$.

RESULTS

Glucose Activates N-WASP, a Downstream Target of Cdc42—Rho GTPase Cdc42 is known to participate in actin dynamics in many eukaryotic cells. To clarify the involvement of Cdc42-mediated F-actin remodeling in GIIS, we first examined the effect of glucose on Cdc42 activation in MIN6-K8 β-cells. The level of Cdc42-GTP was very low at basal state (2.8 mM glucose). Cdc42-GTP was increased 3 min after glucose stimulation (16.7 mM) in MIN6-K8 β-cells and remained at the same level 15 min after stimulation (Fig. 1*A*). In contrast, Cdc42 was not activated by 60 mM K^+ stimulation (Fig. 1*B*). Nifedipine, an L-type voltage-dependent Ca^{2+} channel blocker, did not inhibit glucose-activated Cdc42 in MIN6-K8 β-cells (Fig. 1*C*). These results indicate that Cdc42 in pancreatic β-cells is activated by glucose metabolism, but not by Ca^{2+}.

Because N-WASP is a downstream target of Cdc42 in PC12 cells, COS-7 cells, and breast carcinoma cells (43), we investigated possible glucose inducement of interaction of Cdc42 and N-WASP in MIN6-K8 β-cells. The interaction of N-WASP and Cdc42 was significantly increased 1 min after glucose stimulation, and the increased interaction was maintained during the

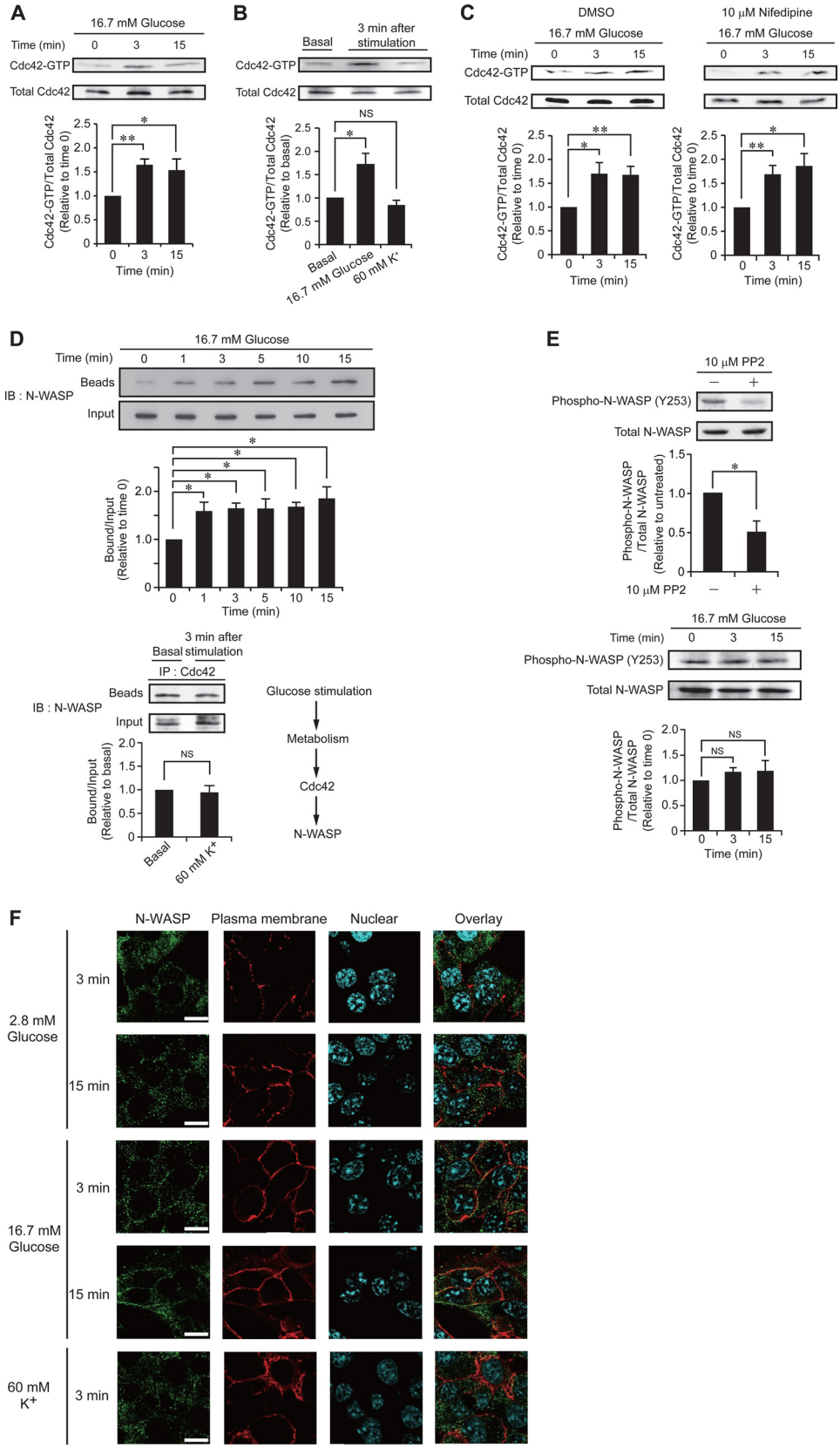

stimulation (Fig. 1*D*, *upper panel*). The interaction was not enhanced by 60 mM K^+ stimulation (Fig. 1*D*, *lower left*). These results indicate that glucose simulation promotes interaction of Cdc42 with N-WASP in pancreatic β-cells (Fig. 1*D*, *lower right*).

Interaction of N-WASP and Cdc42 induces a conformational change of N-WASP, leading to its activation (30). It has been shown that N-WASP at tyrosine 253 (Tyr-253) is phosphorylated by Src family kinases, which induce a conformation change of N-WASP that is important for its activation (44). Indeed, we found that N-WASP at Tyr-253 was phosphorylated at a low level at basal state in MIN6-K8 β-cells and that the phosphorylation was significantly decreased by PP2, a specific inhibitor of the Src family kinases (Fig. 1*E*, *upper panel*). We also found that the phosphorylation was not increased either 3 or 15 min after glucose stimulation (Fig. 1*E, lower panel*). These results indicate that N-WASP is not activated by phosphorylation during glucose stimulation.

We then examined subcellular localization of endogenous N-WASP in MIN6-K8 β-cells and found it to be diffusely localized in MIN6-K8 β-cells at basal state, whereas it was colocalized with mCherry-C*AAX*, a plasma membrane marker, under glucose stimulation (Fig. 1*F*). Stimulation by 60 mM K^+ did not alter subcellular localization of N-WASP. Thus, N-WASP is translocated to the β-cells plasma membrane by glucose stimulation and not by Ca^{2+}. This is consistent with the finding that interaction of N-WASP and Cdc42 is induced by glucose but not by Ca^{2+}.

N-WASP Mediates Glucose-induced Actin Dynamics—Although changes in the cortical actin network have been studied by morphological analyses of fixed cell preparations, there has been no report of visualization of actin dynamics in living pancreatic β-cells. We visualized N-WASP-mediated actin dynamics beneath the plasma membrane in pancreatic β-cells by using G-actin fused to green fluorescent protein AcGFP1 (AcGFP1-actin). A previous study of fixed β-cells using phalloidin-fluorescein isothiocyanate (FITC), which labels F-actin specifically, suggested that glucose induces F-actin remodeling beneath the plasma membrane of MIN6 cells (45). To determine whether N-WASP mediates actin polymerization in β-cells, we utilized a dominant-negative mutant N-WASP lacking the VCA region (N-WASP DN), which cannot bind to either the G-actin or Arp2/3 complex (Fig. 2*A*). We introduced N-WASP DN together with AcGFP1-actin into primary cultured mouse pancreatic β-cells by adenovirus-based gene transfer. Actin dynamics was then visualized by monitoring the fluorescence intensity of AcGFP1-actin detected within 40 nm from the cell surface, by using TIRFM (Fig. 2*B*). The fluorescence intensity of AcGFP1-actin near the plasma membrane was enhanced in mCherry-introduced β-cells (control) and in N-WASP WT-introduced β-cells in the presence of 16.7 mM glucose, whereas introduction of N-WASP DN into β-cells completely blocked enhancement of the fluorescence intensity (Fig. 2*B*). These results suggest that the interaction of N-WASP and Arp2/3 complex mediates glucose-induced actin dynamics beneath the plasma membrane in pancreatic β-cells.

Cdc42/N-WASP/Arp2/3 Complex Signaling Is Required in Glucose-induced Insulin Secretion—We then examined participation of Cdc42 in GIIS from MIN6-K8 β-cells by knockdown experiments. GIIS was decreased in Cdc42 knockdown MIN6-K8 β-cells (Fig. 3*A*), compared with that in control, as reported previously (13). In addition, knockdown of N-WASP in MIN6-K8 β-cells significantly reduced GIIS (Fig. 3*B*). To determine whether N-WASP-mediated actin polymerization was involved in GIIS in β-cells, we utilized N-WASP DN. Introduction of N-WASP DN into MIN6-K8 β-cells significantly reduced GIIS, compared with that from mCherry-introduced or N-WASP WT-introduced MIN6-K8 β-cells, whereas GIIS from N-WASP WT-introduced MIN6-K8 β-cells was not significantly different from that of mCherry-introduced MIN6-K8 β-cells (Fig. 3*C*). To determine whether Arp2/3 complex is critical for GIIS, we examined the effect of knockdown of p34-ARC, a core molecule of Arp2/3 complex, on GIIS. GIIS was decreased in p34-ARC-knockdown MIN6-K8 β-cells, compared with that in control (Fig. 3*D*). Similar results were obtained using mouse pancreatic islets (Fig. 3, *E–G*), further confirming that Cdc42/N-WASP/Arp2/3 complex signal is required for GIIS from pancreatic β-cells.

N-WASP Regulates the Second Phase of Glucose-induced Insulin Secretion—Glucose induces insulin secretion in a biphasic manner. To clarify the role of N-WASP-mediated actin polymerization in biphasic insulin secretion, we performed perifusion experiments using MIN6-K8 β-cells (Fig. 4, *A* and *B*). Knockdown of N-WASP suppressed GIIS, especially in second phase (Fig. 4*A*). In addition, there was no significant difference in biphasic insulin secretion between mCherry-introduced MIN6-K8 β-cells and N-WASP WT-introduced MIN6-K8 β-cells. The first phase of GIIS in N-WASP DN-in-

FIGURE 1. **Glucose-induced activation of Cdc42 and N-WASP.** *A* and *B,* effects of glucose or K^+ stimulation on Cdc42 activation in MIN6-K8 β-cells. MIN6-K8 β-cells were stimulated by 16.7 mM glucose for 0, 3, or 15 min (*A*) or 60 mM K^+ for 3 min (*B*). After stimulation, GTP-bound Cdc42 was affinity-purified by GST pulldown assay and detected with anti-Cdc42 antibody. The *graphs* show the ratio of Cdc42-GTP/total Cdc42. Data are means ± S.E. of three independent experiments. *, $p < 0.05$; **, $p < 0.01$. *C,* effect of nifedipine, an L-type voltage-dependent Ca^{2+} channel blocker, on Cdc42 activation by glucose in MIN6-K8 β-cells. MIN6-K8 β-cells were stimulated by 16.7 mM glucose in the absence or presence of nifedipine (10 μM) for 0, 3, or 15 min. Data are means ± S.E. of three independent experiments. *, $p < 0.05$; **, $p < 0.01$. *D, upper panel,* effects of glucose on the interaction of Cdc42 and its downstream molecule N-WASP. The lysates of MIN6-K8 β-cells after stimulation with glucose for the indicated times were subjected to immunoprecipitation (*IP*) assay with anti-Cdc42 antibody. Western blot analysis with anti-N-WASP antibody was performed. Data are the means ± S.E. of four independent experiments. *, $p < 0.05$; **, $p < 0.01$. *IB,* immunoblot. *D, lower left,* effects of K^+ stimulation on Cdc42/N-WASP interaction. Data are means ± S.E. of three independent experiments. *E, upper panel,* effect of PP2, a specific inhibitor of the Src family kinases, on phosphorylation of N-WASP (Tyr-253). MIN6-K8 β-cells were cultured in the absence or presence of PP2 (10 μM) for 16 h, and the levels of phosphorylated N-WASP were determined with anti-phospho-N-WASP antibody. Data are means ± S.E. of three independent experiments. *, $p < 0.05$. *E, lower panel,* phosphorylation of N-WASP (Tyr-253) in MIN6-K8 β-cells stimulated with glucose. MIN6-K8 β-cells were stimulated by 16.7 mM glucose for the indicated times, and the levels of phosphorylated N-WASP were determined with anti-phospho-N-WASP antibody. Data are means ± S.E. of three independent experiments. *F,* localization of N-WASP in MIN6-K8 β-cells stimulated with 16.7 mM glucose for 3 and 15 min or 60 mM K^+ for 3 min. N-WASP was stained in *green* and nucleus was counterstained with NucRed Live 647 ReadyProbe Reagent (*blue*). Plasma membrane was labeled with mCherry-C*AAX* (*red*). Images were acquired with a confocal microscope. *Bar* indicates 10 μm. Statistical analyses were performed by Student's unpaired *t* test for *D* (*lower panel*) and *E* (*upper panel*) and Tukey's method for *A–D* (*upper panel*) and *E* (*lower panel*). *NS,* not significant in *B, D,* and *E* (*lower panel*).

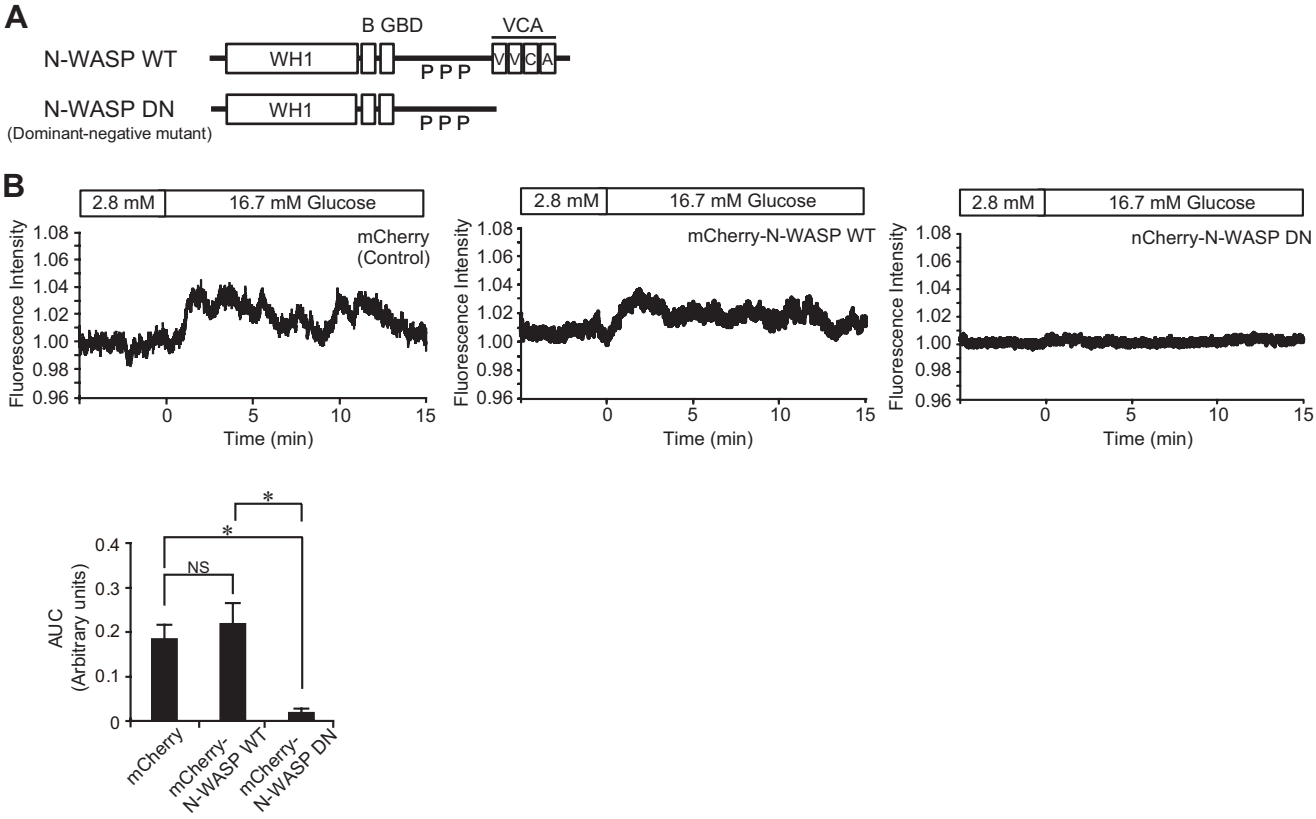

FIGURE 2. **N-WASP-mediated actin dynamics.** *A,* schematic representation of wild-type N-WASP (*N-WASP WT*) and dominant-negative N-WASP mutant (*N-WASP DN*). *WH1,* WASP homology 1 domain; *B,* basic amino acids; *GBD,* GTPase-binding domain; *P,* proline-rich region; *V,* verprolin-homology; *C,* cofilin homology region; and *A,* acidic domain (VCA region). *B*, *upper panel,* change of actin dynamics near plasma membrane of pancreatic β-cells stimulated with glucose. Primary cultured mouse pancreatic β-cells were infected with adenovirus carrying AcGFP1-actin together with mCherry, mCherry-N-WASP WT, or mCherry-N-WASP DN for 2 days. After 30 min of preincubation with 2.8 mM glucose, the fluorescence intensity of AcGFP1-actin near the plasma membrane was monitored in the cells stimulated with 16.7 mM glucose, using TIRFM. Representative data are shown. *B*, *lower panel,* area under the curve (*AUC*) was calculated as the sum of the increase of fluorescence intensity values (0–15 min) compared with basal conditions (at time 0) measured after 16.7 mM glucose stimulation and expressed in arbitrary units. Data are means ± S.E. of 3–5 independent experiments (n = 1–3 for each experiment). *, $p < 0.01$. Statistical analysis was performed by Tukey's method. *NS,* not significant.

troduced MIN6-K8 β-cells was similar to that in N-WASP WT-introduced cells (Fig. 4*B*). In contrast, the second phase of GIIS in N-WASP DN-introduced MIN6-K8 β-cells was significantly reduced, compared with that in mCherry-introduced cells or N-WASP WT-introduced cells (Fig. 4*B*). We further examined the role of N-WASP-induced actin polymerization in insulin granule exocytosis in primary cultured mouse pancreatic β-cells (Fig. 4, *C–F*), using the TIRFM system (11). Insulin granule exocytosis occurs in three different modes based on the dynamics of the insulin granules as follows: 1) *old face*, granules that are predocked to the plasma membrane and fused to the membrane by stimulation; 2) *restless newcomer*, granules that are newly recruited and immediately fused to the plasma membrane by stimulation without docking; and 3) *resting newcomer*, granules that are newly recruited, docked, and fused to the plasma membrane by stimulation. There was no significant difference in the number of docked granules between N-WASP WT-introduced β-cells and N-WASP DN-introduced β-cells (Fig. 4*C*). Both phases of glucose-induced insulin granule exocytosis were caused mainly by *restless newcomer* in N-WASP WT-introduced β-cells (Fig. 4 *D*, *upper panel,* and *F*). The number of fusion events in the first phase in N-WASP DN-introduced β-cells was similar to that in N-WASP WT-introduced β-cells (Fig. 4, *D–F*). In contrast, the number of fusion events in the second phase was significantly reduced in N-WASP DN-introduced β-cells (Fig. 4, *D–F*), a finding consistent with those obtained by perifusion experiments (Fig. 4*B*). These results demonstrate that actin polymerization regulated by Cdc42/N-WASP signal is required in the second phase of GIIS by facilitating recruitment of *restless newcomer*.

Glucose Enhances Phosphorylation of Cofilin That Initiates F-actin Remodeling—Because PAK1 is also a downstream target of Cdc42 (43), we examined the effect of glucose stimulation on the interaction of Cdc42 and PAK1 in MIN6-K8 β-cells. The interaction was significantly enhanced 3 and 15 min after glucose stimulation (Fig. 5*A*, *left* and *middle panels*), although the interaction was not enhanced by 60 mM K^+ stimulation (Fig. 5*A*, *right panel*). PAK1 activates LIM kinase 1 (LIMK1) by its phosphorylation (46), which phosphorylates cofilin at serine 3. Phosphorylation of cofilin (inactive form) inhibits its actin depolymerizing activity by binding to actin monomers (47, 48). Dephosphorylated cofilin (active form) increases the rate of actin depolymerization and maintains a pool of actin monomer (33). We found that phosphorylation of LIMK1 is induced by glucose stimulation but is not phosphorylated by K^+ stimulation (Fig. 5*B*). We therefore examined whether glucose stimulation (16.7 mM) increases phosphorylation of cofilin in MIN6-K8 β-cells. The level of phosphorylated cofilin was grad-

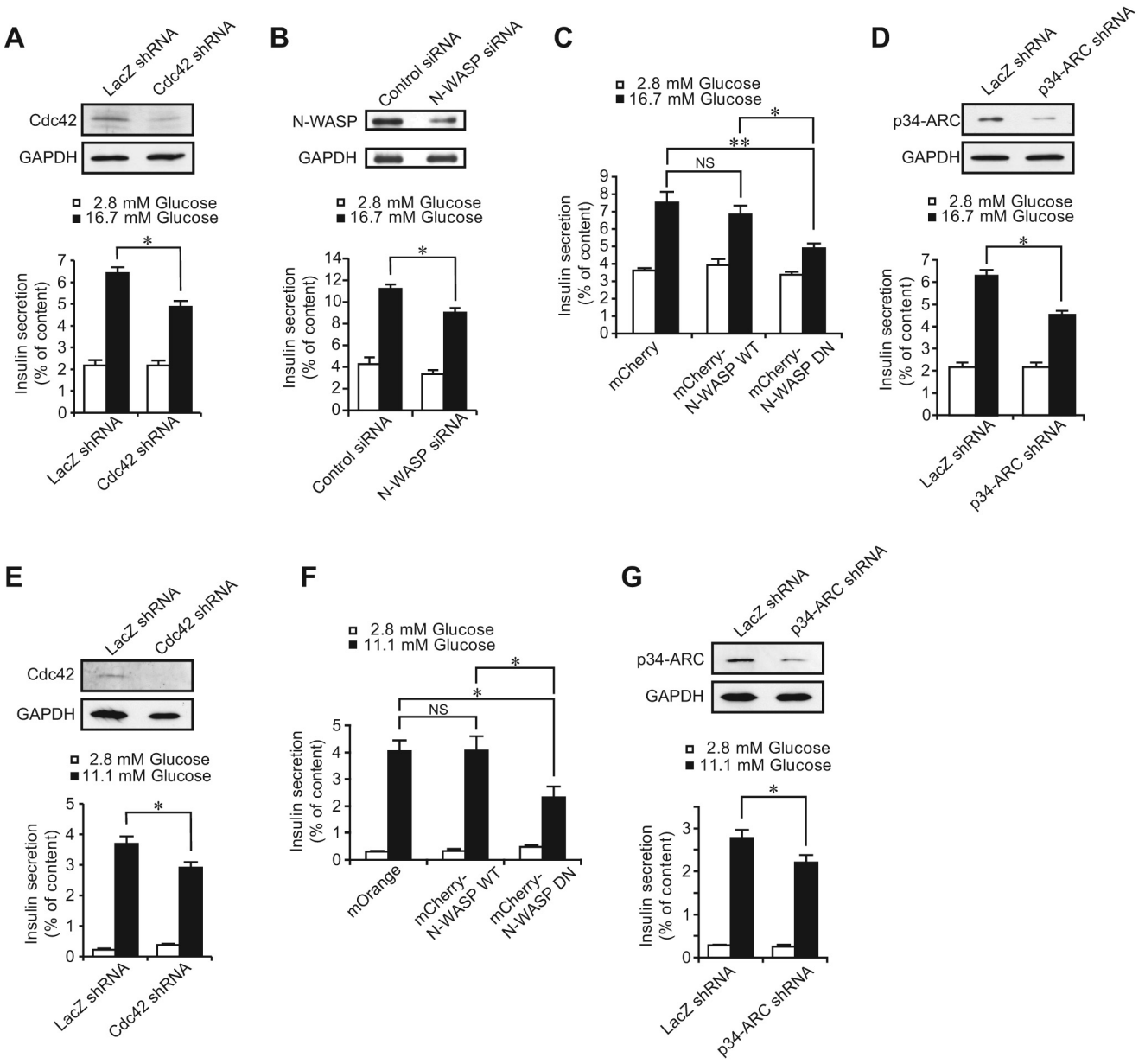

FIGURE 3. **Effect of Cdc42/N-WASP signaling on insulin secretion.** *A*, effects of Cdc42 knockdown on insulin secretion in MIN6-K8 β-cells. MIN6-K8 β-cells were infected with adenovirus carrying LacZ shRNA or Cdc42 shRNA. After 30 min of preincubation, MIN6-K8 β-cells were stimulated by 16.7 mM glucose for 30 min. Data are means ± S.E. of three independent experiments ($n = 4–8$ for each experiment). *, $p < 0.005$. *B*, effects of N-WASP knockdown on insulin secretion in MIN6-K8 β-cells. Control siRNA or N-WASP siRNA was transfected into MIN6-K8 β-cells. After 30 min of preincubation, MIN6-K8 β-cells were stimulated by 16.7 mM glucose for 30 min. Data are means ± S.E. of three independent experiments ($n = 4$ for each experiment). *, $p < 0.01$. *C*, effects of N-WASP DN on insulin secretion in MIN6-K8 β-cells. MIN6-K8 β-cells were infected with adenovirus carrying mCherry, mCherry-N-WASP WT, or mCherry-N-WASP DN. After 30 min of preincubation, MIN6-K8 β-cells were stimulated by 16.7 mM glucose for 30 min. Data are means ± S.E. of three independent experiments ($n = 3–7$ for each experiment). *, $p < 0.05$; **, $p < 0.001$. *D*, effects of p34-ARC knockdown on insulin secretion in MIN6-K8 β-cells. MIN6-K8 β-cells were infected with adenovirus carrying LacZ shRNA or p34-ARC shRNA. After 30 min of preincubation, MIN6-K8 β-cells were stimulated by 16.7 mM glucose for 30 min. Data are means ± S.E. of three independent experiments ($n = 4–8$ for each experiment). *, $p < 0.001$. *E*, effects of Cdc42 knockdown on insulin secretion from mouse islets. Isolated mouse islets were infected with adenovirus carrying LacZ shRNA or Cdc42 shRNA. After 30 min of preincubation, mouse islets were stimulated by 11.1 mM glucose for 30 min. Data are means ± S.E. of three independent experiments ($n = 4–8$ for each experiment). *, $p < 0.05$. *F*, effects of N-WASP DN on insulin secretion from mouse islets. Isolated mouse islets were infected with adenovirus carrying mCherry, mCherry-N-WASP WT, or mCherry-N-WASP DN. After 30 min of preincubation, mouse islets were stimulated by 11.1 mM glucose for 30 min. Data are means ± S.E. of three independent experiments ($n = 3–7$ for each experiment). *, $p < 0.05$. *G*, effects of p34-ARC knockdown on insulin secretion from mouse islets. Isolated mouse islets were infected with adenovirus carrying LacZ shRNA or p34-ARC shRNA. After 30 min of preincubation, mouse islets were stimulated by 11.1 mM glucose for 30 min. Data are means ± S.E. of three independent experiments ($n = 4–8$ for each experiment). *, $p < 0.05$. Statistical analyses were performed by Student's unpaired *t* test for *A, B, D, E*, and *G* and Tukey's method for *C* and *F*. *NS*, not significant in *C* and *F*.

ually increased by glucose stimulation in a time-dependent manner (Fig. 5*C*, *left panel*). In contrast, the level of phosphorylated cofilin was decreased by K^+ stimulation (Fig. 5*C*, *right panel*). Cofilin is also known to be phosphorylated at serine 3 by LIMK2, which is an isoform of LIMK1 (46). LIMK2 is activated by its phosphorylation of Rho kinase ROCK (49). However, it is not known whether cofilin is phosphorylated by ROCK/LIMK2 in pancreatic β-cells stimulated with glucose. We examined

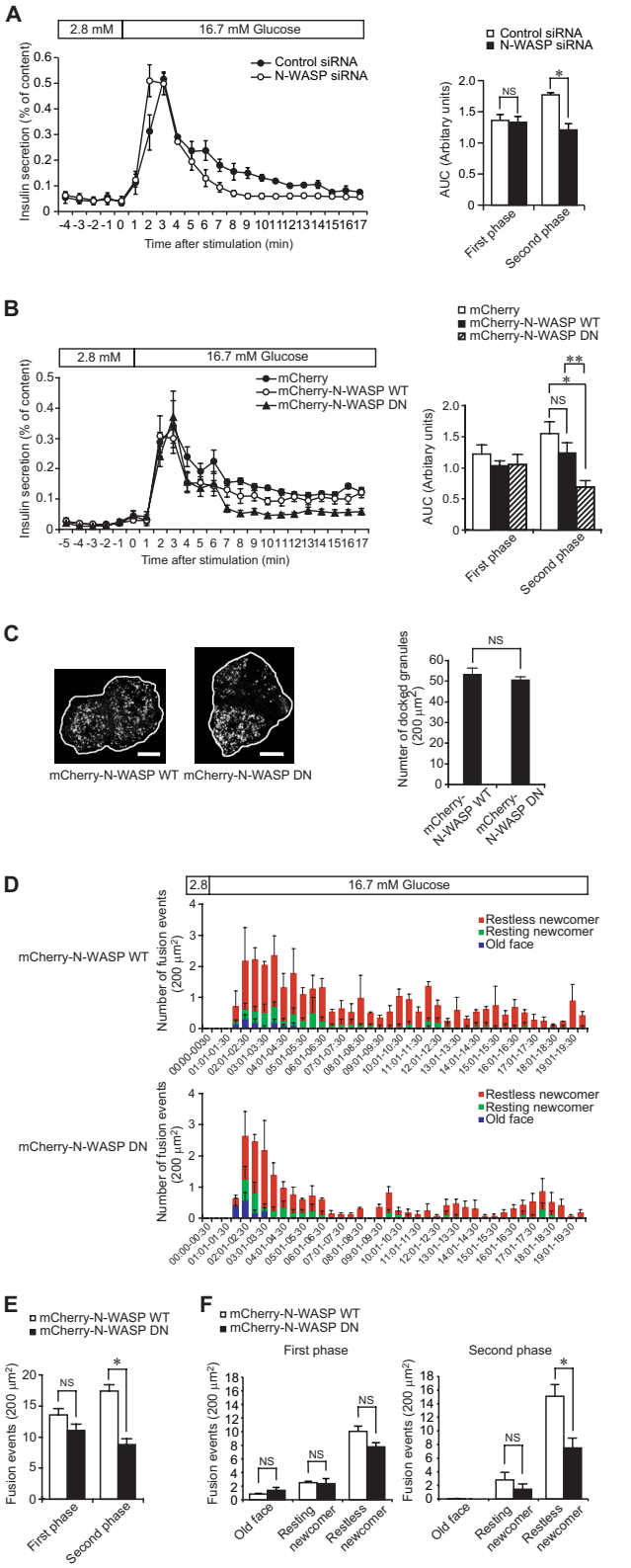

FIGURE 4. **Effects of N-WASP knockdown and N-WASP DN on dynamics of insulin secretion.** *A, left panel,* effects of N-WASP knockdown on insulin secretion in perifused MIN6-K8 β-cells. MIN6-K8 β-cells ware transfected with control siRNA or N-WASP siRNA. After 30 min of preincubation, MIN6-K8 β-cells were stimulated by 16.7 mM glucose for 30 min. Data are means ± S.E. of three independent experiments (n = 1–2 for each experiment). *A, right panel,* comparison of AUC in the first phase (the first 5 min after stimulation) and second phase (from 5–17 min after glucose stimulation) in cells transfected with control siRNA or N-WASP siRNA. Data are expressed as means ± S.E. *, $p < 0.01$. *B, left panel,* effects of N-WASP DN on insulin secretion in perifused MIN6-K8 β-cells. MIN6-K8 β-cells were infected with adenovirus carrying mCherry, mCherry-N-WASP WT, or mCherry-N-WASP DN. After 30 min of preincubation, MIN6-K8 β-cells were stimulated by 16.7 mM glucose for 30 min. Data are means ± S.E. of four independent experiments (n = 1–3 for each experiment). *B, right panel,* comparison of AUC in the first phase (the first 5 min after stimulation) and second phase (from 5 to 17 min after glucose stimulation) in cells overexpressing mCherry, mCherry-N-WASP WT, or mCherry-N-WASP DN. Data are expressed as means ± S.E. *, $p < 0.01$; **, $p < 0.05$. *C, left panel,* insulin granules docked to the plasma membrane in primary cultured mouse pancreatic β-cells infected with adenovirus carrying insulin-Venus together with mCherry-N-WASP WT or mCherry-N-WASP DN. Insulin-Venus-containing granules were observed by TIRFM. The surrounding lines represent the outline of a cell attached to the cover glass. *C, right panel,* comparison of the number of insulin granules docked to the plasma membrane in pancreatic β-cells overexpressing mCherry-N-WASP WT and mCherry-N-WASP DN. The number of docked granules was measured in a cell surface area of 200 μm^2. *Scale bar,* 10 μm. Data are means ± S.E. of three independent experiments. *D, histogram* of fusion events in primary cultured pancreatic β-cells infected with insulin-Venus together with mCherry-N-WASP WT (*upper panel*) or mCherry-N-WASP DN (*lower panel*) in a cell surface area of 200 μm^2. After 30 min of preincubation, primary cultured pancreatic β-cells were stimulated by 16.7 mM glucose. *2.8* indicates 2.8 mM glucose. *Blue, red,* and *green bars* indicate *old face*, *restless newcomer*, and *resting newcomer*, respectively. Data are means ± S.E. of 4–5 independent experiments (n = 1–2 for each experiment). *E*, comparison of fusion events in the first and second phases between mCherry-N-WASP WT and mCherry-N-WASP DN-introduced pancreatic β-cells. The sum of fusion events in the first phase (the first 5 min after glucose stimulation) and that in the second phase (from 5 to 20 min after glucose stimulation) are shown. *F*, distribution of three modes of fusion events in the first phase (*left panel*) and the second phase (*right panel*). *, $p < 0.05$. Data are expressed as means ± S.E. Statistical analyses were performed by Student's unpaired t test for *A, C, E,* and *F* and Tukey's method for *B*, respectively. *NS,* not significant in *A, B, C, E,* and *F*.

mRNA expression levels of LIMK1 and LIMK2 in MIN6-K8 β-cells by real time PCR analysis. We found that LIMK1 and LIMK2 are equally expressed in MIN6-K8 β-cells (Fig. 5*D*). We then examined whether ROCK/LIMK2 phosphorylates cofilin in a glucose-dependent manner. For this purpose, we utilized ROCK inhibitor Y27632 and PAK1 inhibitor IPA3 (Fig. 5*E*, *upper panel*). Phosphorylation levels of cofilin were inhibited by IPA3 in MIN6-K8 β-cells stimulated with glucose (16.7 mM), whereas they were not inhibited by Y27632, suggesting that cofilin is not phosphorylated by ROCK/LIMK2 (Fig. 5*E*, *lower left*). These results indicate that glucose stimulation induces phosphorylation and inactivation of cofilin through activation of Cdc42/PAK1/LIMK1 signaling (Fig. 5*E*, *lower right*).

Cofilin Regulates the Second Phase of Glucose-induced Insulin Secretion—To clarify the role of cofilin in insulin secretion, we performed insulin secretion experiments, using cofilin siRNA. Knockdown of cofilin in MIN6-K8 β-cells significantly reduced GIIS (Fig. 6*A*). To clarify the role of cofilin in dynamics of GIIS, we performed perifusion experiments using MIN6-K8 β-cells. The first phase of GIIS in cofilin knockdown MIN6-K8 β-cells was similar to that in control cells (Fig. 6*B*). In contrast, the second phase of GIIS in cofilin knockdown MIN6-K8 β-cells was significantly reduced, compared with that in control cells (Fig. 6*B*).

We next examined whether cofilin activity is involved in insulin secretion. For this purpose, we utilized cofilin S3D mutant-mimicking phosphorylated form (*i.e.* inactive form) (38). Cofilin S3D mutant competitively acts on the binding of phosphorylated endogenous cofilin to its specific phosphatase, thereby inactivating endogenous cofilin, which inhibits actin polymerization (50). In cofilin S3D-introduced MIN6-K8 β-cells, GIIS was significantly reduced, compared with that in

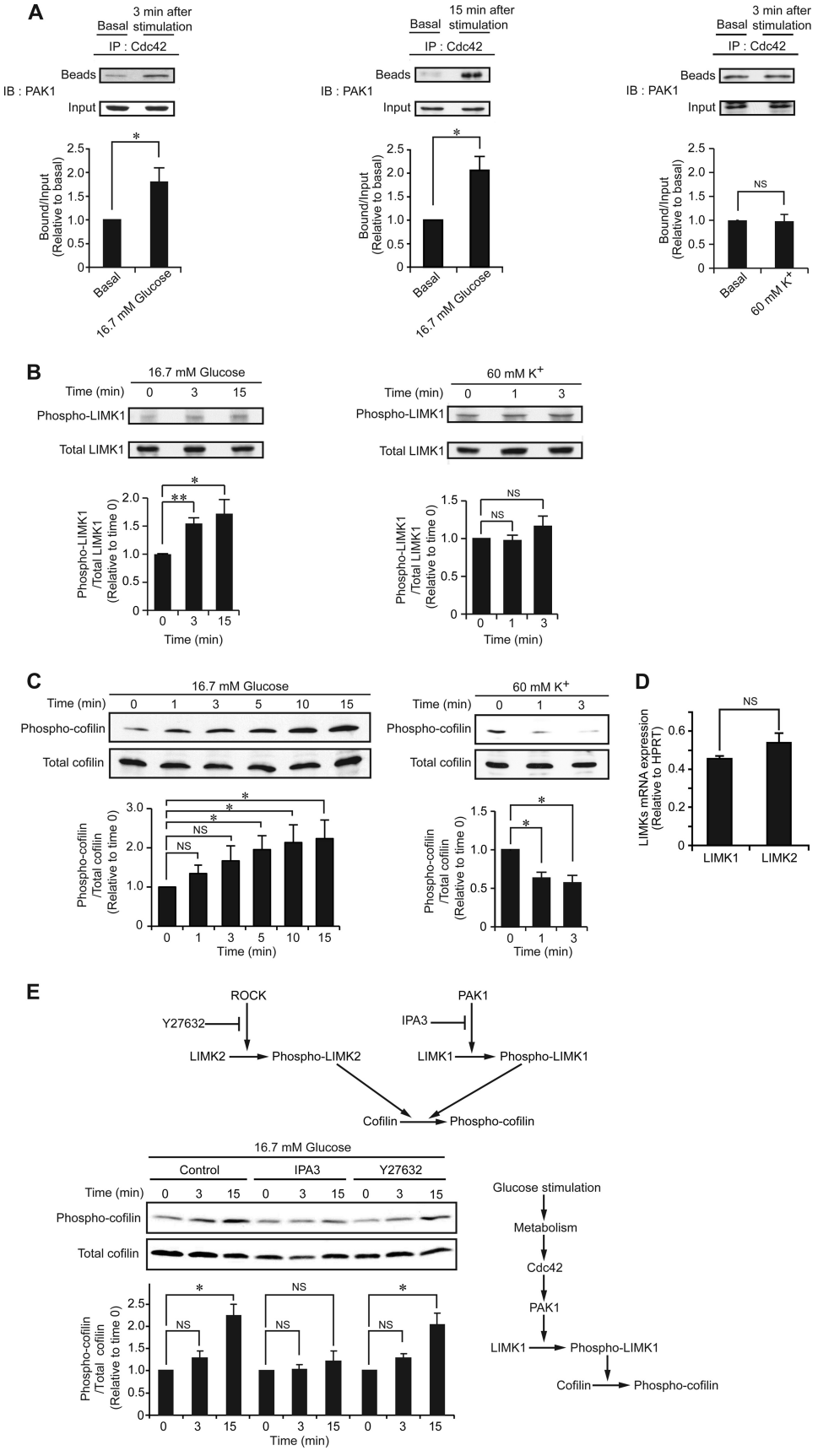
A
3 min after stimulation
Basal
IP : Cdc42
Beads
IB : PAK1
Input
Bound/Input (Relative to basal)
Basal
16.7 mM Glucose
15 min after stimulation
60 mM K+
B
16.7 mM Glucose
60 mM K+
Time (min)
Phospho-LIMK1
Total LIMK1
Phospho-LIMK1 /Total LIMK1 (Relative to time 0)
NS
C
Phospho-cofilin
Total cofilin
Phospho-cofilin /Total cofilin (Relative to time 0)
D
LIMKs mRNA expression (Relative to HPRT)
LIMK1
LIMK2
E
ROCK
Y27632
PAK1
IPA3
LIMK2
Phospho-LIMK2
LIMK1
Phospho-LIMK1
Cofilin
Phospho-cofilin
Control
IPA3
Y27632
Glucose stimulation
Metabolism
Cdc42
PAK1

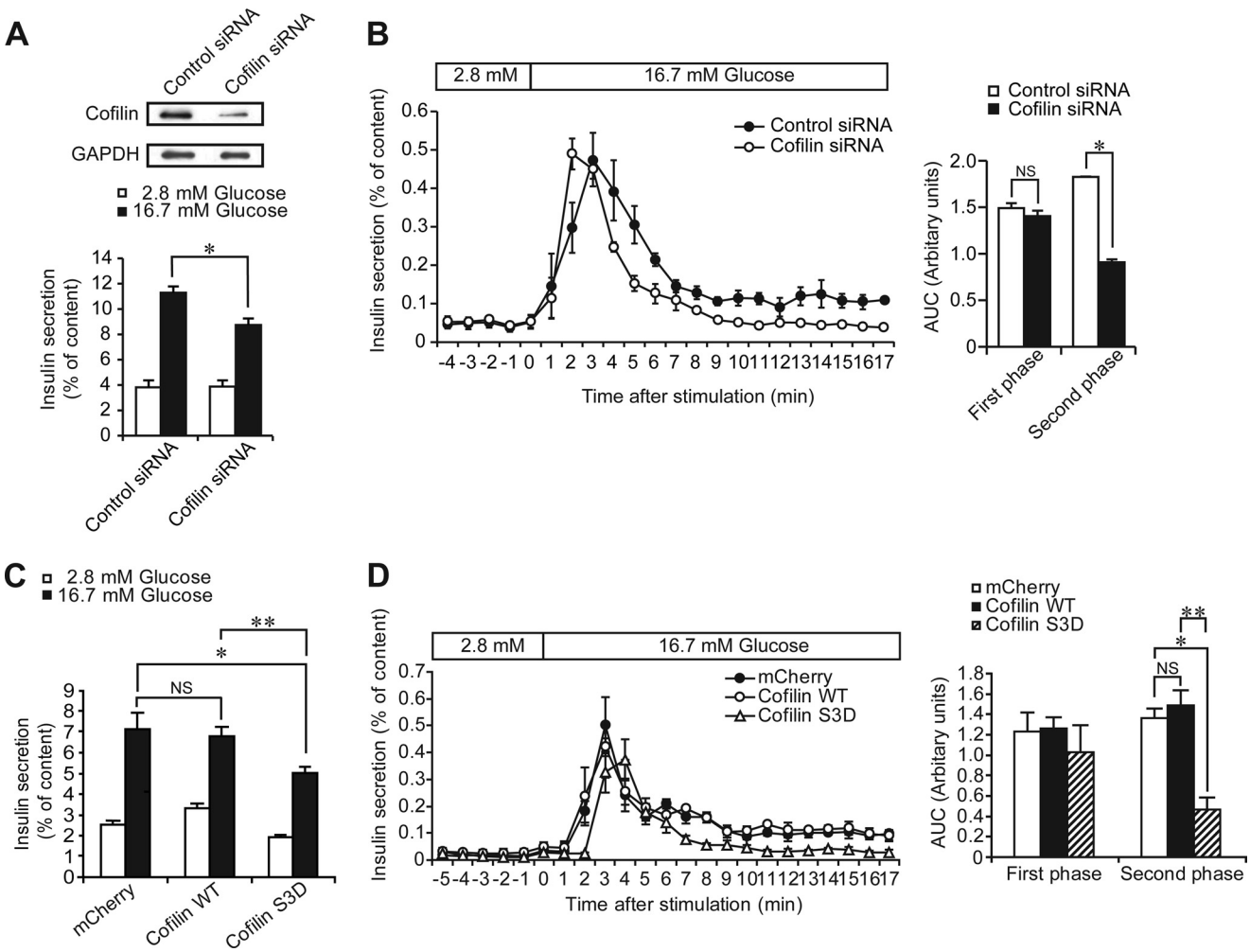

FIGURE 6. **Effect of cofilin knockdown and cofilin S3D mutant on dynamics of insulin secretion.** *A*, effects of cofilin knockdown on insulin secretion in MIN6-K8 β-cells. MIN6-K8 β-cells were transfected with control siRNA or cofilin siRNA. After 30 min of preincubation, MIN6-K8 β-cells were stimulated by 16.7 mM glucose for 30 min. Data are means ± S.E. of three independent experiments ($n = 4$ for each experiment). *, $p < 0.01$. *B, left panel,* effects of cofilin knockdown on insulin secretion in perifused MIN6-K8 β-cells. MIN6-K8 β-cells were transfected with control siRNA or cofilin siRNA. Data are means ± S.E. of three independent experiments ($n = 1$–2 for each experiment). *B, right panel,* comparison of AUC in the first phase (the first 5 min after stimulation) and second phase (from 5 to 17 min after glucose stimulation) in cells transfected with control siRNA or cofilin siRNA. Data are expressed as means ± S.E. *, $p < 0.01$. *C*, effects of cofilin S3D mutant on insulin secretion in MIN6-K8 β-cells. MIN6-K8 β-cells were infected with adenovirus carrying mCherry, cofilin WT, or cofilin S3D. After 30 min of preincubation, MIN6-K8 β-cells were stimulated by 16.7 mM glucose for 30 min. Data are means ± S.E. of four independent experiments ($n = 5$–8 for each experiment). *, $p < 0.05$; **, $p < 0.01$. *D, left panel,* effects of cofilin S3D mutant on insulin secretion in perifused MIN6-K8 β-cells. MIN6-K8 β-cells were infected with adenoviruses carrying mCherry, cofilin WT, or cofilin S3D. Data are means ± S.E. of two independent experiments ($n = 2$–3 for each experiment). *D, right panel,* comparison of AUC in the first phase (the first 5 min after stimulation) and second phase (from 5 to 17 min after glucose stimulation) in cells expressing mCherry, cofilin WT, or cofilin S3D. Data are expressed as means ± S.E. *, $p < 0.05$; **, $p < 0.01$. Statistical analyses were performed by Student's unpaired *t* test for *A* and *B* and Tukey's method for *C* and *D*, respectively. *NS,* not significant in *B, C,* and *D*.

cofilin WT-introduced MIN6-K8 β-cells (Fig. 6*C*). The effect of cofilin S3D mutant on the dynamics of GIIS was also examined by perifusion experiments. The first phase of GIIS in cofilin S3D-introduced MIN6-K8 β-cells was similar to that in cofilin WT-introduced MIN6-K8 β-cells, whereas the second phase in cofilin S3D-introduced MIN6-K8 β-cells was decreased signif-

FIGURE 5. **Phosphorylation of LIMK1 and cofilin by glucose.** *A, left* and *middle panels,* effects of glucose on the interaction of Cdc42 and its downstream molecule PAK1. The lysates of MIN6-K8 β-cells after stimulation with glucose for 3 min (*left panel*) or 15 min (*middle panel*) were subjected to immunoprecipitation (*IP*) assay with anti-Cdc42 antibody. Western blot analysis with anti-PAK1 antibody was performed. Data are means ± S.E. of 4–5 independent experiments. *, $p < 0.05$. *IB,* immunoblot. *A, right panel,* effects of K^+ stimulation on Cdc42/PAK1 interaction. Data are means ± S.E. of four independent experiments. *B*, effects of glucose (*left panel*) or K^+ (*right panel*) stimulation on LIMK1 phosphorylation (threonine 508) in MIN6-K8 β-cells. The lysates of MIN6-K8 β-cells after stimulation with glucose or K^+ for indicated times were subjected to Western blot analysis with anti-phospho-LIMK1 or anti-LIMK1 antibody. Data are means ± S.E. of four independent experiments. *, $p < 0.05$; **, $p < 0.01$. *C*, effects of glucose (*left panel*) or K^+ (*right panel*) stimulation on cofilin phosphorylation (serine 3) in MIN6-K8 β-cells. The lysates of MIN6-K8 β-cells after stimulation with glucose or K^+ for the indicated times were subjected to Western blot analysis with anti-phospho-cofilin or anti-cofilin antibody. Data are means ± S.E. of four independent experiments. *, $p < 0.01$. *D*, comparison of LIMK1 and LIMK2 mRNA expression levels in MIN6-K8 β-cells. Data are means ± S.E. of three independent experiments. *E*, effects of IPA3, a PAK1 inhibitor, or Y27632, a ROCK inhibitor, on cofilin phosphorylation in MIN6-K8 β-cells. The lysates of MIN6-K8 β-cells after stimulation with glucose in the presence of IPA3 (30 μM) or Y27632 (10 μM) for the indicated times were subjected to Western blot analysis with anti-phospho-cofilin or anti-cofilin antibody. Data are means ± S.E. of four independent experiments ($n = 5$–8 for each experiment). *, $p < 0.05$; **, $p < 0.01$. Statistical analyses were performed by Student's unpaired *t* test for *A* and *D* and Tukey's method for *B, C,* and *E*, respectively. *NS,* not significant in *A–E*.

icantly (Fig. 6*D*), indicating that activity of cofilin is critical for the second phase of GIIS.

DISCUSSION

Actin dynamics has recently emerged as a key event in vesicle trafficking in exocytosis and endocytosis (17, 51). In chromaffin cells and their derived PC12 cells, actin forms a complex and dynamic network of filaments beneath the plasma membrane, and rapid remodeling of the actin network is required for exocytosis of catecholamine (52). In 3T3-L1 adipocytes, remodeling of cortical actin at the plasma membrane is a necessary and rate-limiting step for fusion of GLUT4 vesicles (53). Although roles of the actin network in insulin secretion from pancreatic β-cells have been investigated by pharmacological and morphological approaches, the dynamics of actin in living pancreatic β-cells has not been described. In this study, we investigated the mechanism of glucose regulation of actin dynamics regulated by N-WASP and cofilin, which are the major regulators of actin dynamics, and its role in the biphasic response of GIIS. We first established a system using a combination of AcGFP1-labeled actin and TIRFM to visualize actin dynamics of living β-cells. We found that glucose induces actin dynamics in primary cultured pancreatic β-cells that is completely blocked by inactivation of N-WASP. In PC12 cells, the Ca^{2+} signal initiates the interaction of Cdc42 and N-WASP, leading to actin polymerization and triggering of catecholamine release (54). However, the Ca^{2+} signal in pancreatic β-cells does not activate Cdc42 and does not induce interaction of Cdc42 with N-WASP or PAK1. In contrast, glucose induces interaction of Cdc42 with N-WASP or PAK1. Cdc42 activation also requires glucose metabolism (13). Thus, glucose metabolism rather than the Ca^{2+} signal is essential for activation of the Cdc42/N-WASP/Arp2/3 complex signal and the Cdc42/PAK1/LIMK1/cofilin signal in pancreatic β-cells.

Phosphorylation of N-WASP at tyrosine 253 by Src family kinases has been shown to cause its activation in neuronal cells (55). However, our data reveal that N-WASP is not activated by phosphorylation at tyrosine 253 by glucose stimulation in MIN6-K8 β-cells. We also found that Cdc42 activates PAK1 by glucose stimulation. It has been shown that activated PAK1 phosphorylates LIMK1 (46) and that phosphorylated LIMK1 phosphorylates cofilin (*i.e.* inactivates cofilin), which decreases its actin depolymerizing activity (47, 48). In addition, we found that phosphorylations of LIMK1 and cofilin are induced by glucose stimulation in MIN6-K8 β-cells.

Because Cdc42 binds to N-WASP and PAK1, the three proteins might form a complex. However, it has been shown that WASP and PAK bind to the same region in Cdc42 (56), suggesting that the complex cannot be formed. The distinct pools comprising Cdc42/N-WASP/Arp2/3 complex signal and Cdc42/PAK1/LIMK1/cofilin signal could well be involved in control of glucose-induced actin dynamics.

We recently found that both the first phase and the second phase of GIIS are caused by insulin granules that are newly recruited and immediately fused to the plasma membrane without docking (*restless newcomer*) (11, 41), but the mechanisms underlying biphasic insulin secretion remain unclear. At basal state (2.8 mM glucose, nonstimulated condition), most of the cofilin is present in its dephosphorylated form (active form), which severs F-actin. As a result, at basal state, G-actin predominates over F-actin. Glucose stimulation drastically alters the states of G-actin and F-actin by changing cofilin and N-WASP activities in a time-dependent manner. In the early period ($<$ ~5 min) during glucose stimulation, which corresponds to the first phase of GIIS, the level of phosphorylated cofilin (inactive form) is gradually increased, but the majority of cofilin is still dephosphorylated in this period. The activity of cofilin therefore predominates over the activity of the N-WASP/Arp2/3 complex, thereby severing the remodeled F-actin and resulting in a G-actin predominant state. In accord with this, a recent study reports that glucose stimulation (20 mM) decreases the amount of F-actin near the plasma membrane within 5 min, compared with that at basal state (glucose-free), and recovers it in 30 min (45). Considered together, these findings suggest that, in contrast to the later period, insulin granules in first phase glucose stimulation undergo undirected trafficking from RRP, independent of the actin network, and are immediately fused to the plasma membrane. This may account for the characteristic dynamics of first phase of GIIS, which occurs rapidly, massively, and transiently. Indeed, actin-depolymerizing agents such as cytochalasin B and latrunculin B sustain massive insulin secretion from perifused pancreatic islets during application (23, 45, 57). It is also established that insulin is immediately, massively, and transiently secreted by K^+ stimulation (6, 8). We found that K^+ stimulation did not cause activation of Cdc42 in pancreatic β-cells, confirming a previous report (25), and that N-WASP was not activated by K^+ stimulation. Interestingly, in contrast to the effect of glucose stimulation, the level of phosphorylated cofilin was decreased significantly by K^+ stimulation, compared with its basal level, indicating that the F-actin-severing activity of cofilin is enhanced during stimulation. These findings indicate that a G-actin-predominant state is associated closely with immediate, massive, and transient response of insulin granule exocytosis. However, in the late period ($>$ ~5 min) during glucose stimulation, which corresponds to the second phase of GIIS, the level of phosphorylated cofilin reaches nearly maximum 5 min after stimulation and is sustained thereafter. In contrast, N-WASP is rapidly activated, and its activity is sustained throughout glucose stimulation. Thus, activity of the N-WASP/Arp2/3 complex signal predominates over that of cofilin in the late period, thereby effecting F-actin remodeling. Indeed, introduction of an N-WASP DN into MIN6-K8 β-cells or N-WASP knockdown disclosed a marked decrease of the second phase of GIIS, as assessed by perifusion experiments. These findings are consistent with the recent studies showing that the second phase of GIIS was decreased in perifused Cdc42 knockdown islets and islets isolated from PAK1 knock-out mice (13, 58). A cofilin DN is known to inhibit the supply of G-actin that is essential for actin polymerization by blocking endogenous cofilin (50). We found that introduction of cofilin DN into MIN6-K8 β-cells also decreases the second phase of GIIS. Given that both N-WASP DN and cofilin DN inhibit the second phase of GIIS, F-actin remodeling is clearly regulated by activities of N-WASP and cofilin in pancreatic β-cells and is essential for the second phase of GIIS. The second phase of GIIS is caused almost exclusively by *restless newcomer* (11); F-actin

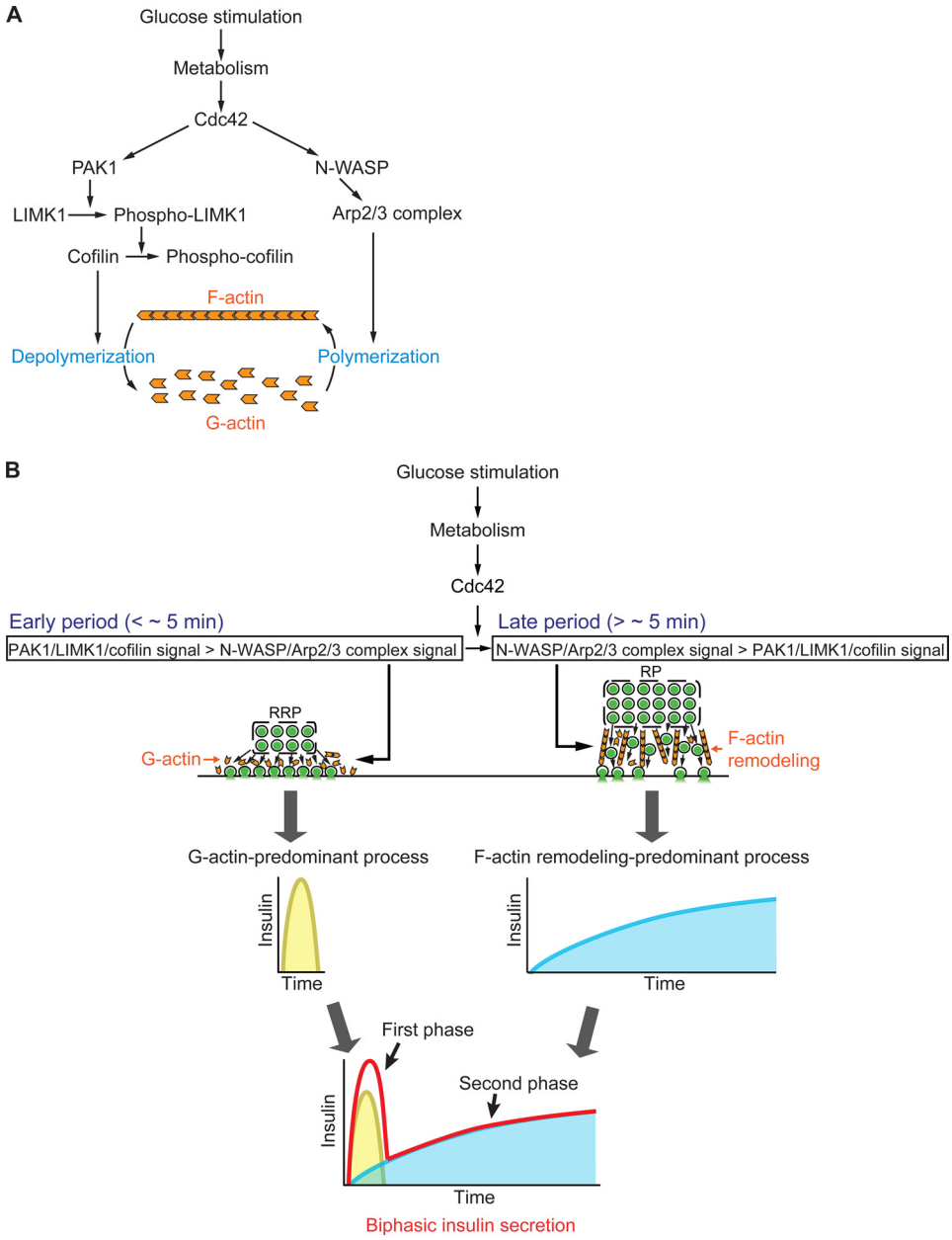

FIGURE 7. **Model for the relationship between actin dynamics and biphasic insulin secretion by glucose.** *A*, glucose simulation promotes interaction of Cdc42 with both PAK1 and N-WASP and activates them through glucose metabolism in pancreatic β-cells. PAK1 activates LIMK1 by its phosphorylation. Activated LIMK1 phosphorylates and inactivates cofilin, which severs F-actin. N-WASP induces actin polymerization through its interaction with the Arp2/3 complex. Glucose stimulation triggers F-actin remodeling through Cdc42/PAK1/LIMK1/cofilin signal and Cdc42/N-WASP/Arp2/3 complex signal. *B*, glucose induces insulin secretion by G-actin predominant process (*yellow*) and F-actin remodeling predominant process (*blue*). In the early period (< ~5 min) after glucose stimulation, cofilin activity, which severs F-actin, predominates over N-WASP activity. In this period, insulin secretion from readily releasable pool (*RRP*) near the plasma membrane occurs rapidly, massively, and transiently. In the late period (> ~ 5 min), N-WASP activity predominates over cofilin activity, thereby effecting the F-actin remodeling that facilitates trafficking of insulin granules from RP to the plasma membrane. G-actin predominant process and F-actin remodeling predominant process occur concurrently after glucose stimulation. The first phase of GIIS consists of the sum of insulin secretion due to both G-actin predominant process and F-actin remodeling predominant process, the former being major. However, the second phase of GIIS consists primarily of insulin secretion caused by the F-actin remodeling predominant process.

remodeling might control or otherwise facilitate trafficking of these insulin granules to the plasma membrane, where fusion events can occur.

We propose a model of the relationship between actin dynamics and the biphasic response of GIIS (Fig. 7). The first phase of GIIS is associated with insulin secretion mostly by the G-actin predominant process, in which the Cdc42/PAK1/LIMK1/cofilin signal is predominant. However, the second phase of GIIS is associated mostly with insulin secretion caused by the F-actin remodeling predominant process, in which the Cdc42/N-WASP/Arp2/3 complex signal is predominant. Thus, actin dynamics regulated by the balance between N-WASP and cofilin activities is critical in determining the biphasic response of GIIS.

As impaired dynamics of insulin secretion is a characteristic feature of diabetes (59, 60), it is important to clarify the roles of N-WASP and cofilin in the pathogenesis and pathophysiology of diabetic β-cells.

Acknowledgments—We thank J. Condeelis (Albert Einstein College of Medicine, New York) for providing us with N-WASP cDNA. We also thank G. K. Honkawa (Kobe University Graduate School of Medicine, Kobe, Japan) for assistance in preparing the manuscript.

REFERENCES

1. Porte, D., Jr., and Kahn, S. E. (1991) Mechanisms for hyperglycemia in type II diabetes mellitus: therapeutic implications for sulfonylurea treatment–an update. *Am. J. Med.* **90,** 8S-14S
2. Polonsky, K. S., Sturis, J., and Bell, G. I. (1996) Seminars in Medicine of the Beth Israel Hospital, Boston. Non-insulin-dependent diabetes mellitus–a genetically programmed failure of the β cell to compensate for insulin resistance. *N. Engl. J. Med.* **334,** 777–783
3. Kahn, S. E., Montgomery, B., Howell, W., Ligueros-Saylan, M., Hsu, C. H., Devineni, D., McLeod, J. F., Horowitz, A., and Foley, J. E. (2001) Importance of early phase insulin secretion to intravenous glucose tolerance in subjects with type 2 diabetes mellitus. *J. Clin. Endocrinol. Metab.* **86,** 5824–5829
4. Henquin, J. C. (2009) Regulation of insulin secretion: a matter of phase control and amplitude modulation. *Diabetologia* **52,** 739–751
5. Curry, D. L., Bennett, L. L., and Grodsky, G. M. (1968) Dynamics of insulin secretion by the perfused rat pancreas. *Endocrinology* **83,** 572–584
6. Henquin, J. C., Ishiyama, N., Nenquin, M., Ravier, M. A., and Jonas, J. C. (2002) Signals and pools underlying biphasic insulin secretion. *Diabetes* **51,** S60–67
7. Eliasson, L., Abdulkader, F., Braun, M., Galvanovskis, J., Hoppa, M. B., and Rorsman, P. (2008) Novel aspects of the molecular mechanisms controlling insulin secretion. *J. Physiol.* **586,** 3313–3324
8. Rorsman, P., and Renström, E. (2003) Insulin granule dynamics in pancreatic β cells. *Diabetologia* **46,** 1029–1045
9. Barg, S., Eliasson, L., Renström, E., and Rorsman, P. (2002) A subset of 50 secretory granules in close contact with L-type Ca^{2+} channels accounts for first-phase insulin secretion in mouse β-cells. *Diabetes* **51,** S74-S82
10. Straub, S. G., Shanmugam, G., and Sharp, G. W. (2004) Stimulation of insulin release by glucose is associated with an increase in the number of docked granules in the β-cells of rat pancreatic islets. *Diabetes* **53,** 3179–3183
11. Shibasaki, T., Takahashi, H., Miki, T., Sunaga, Y., Matsumura, K., Yamanaka, M., Zhang, C., Tamamoto, A., Satoh, T., Miyazaki, J., and Seino, S. (2007) Essential role of Epac2/Rap1 signaling in regulation of insulin granule dynamics by cAMP. *Proc. Natl. Acad. Sci. U.S.A.* **104,** 19333–19338
12. Seino, S., Shibasaki, T., and Minami, K. (2011) Dynamics of insulin secretion and the clinical implications for obesity and diabetes. *J. Clin. Invest.* **121,** 2118–2125
13. Wang, Z., Oh, E., and Thurmond, D. C. (2007) Glucose-stimulated Cdc42 signaling is essential for the second phase of insulin secretion. *J. Biol. Chem.* **282,** 9536–9546
14. Wang, Z., and Thurmond, D. C. (2009) Mechanisms of biphasic insulin-granule exocytosis–roles of the cytoskeleton, small GTPases and SNARE proteins. *J. Cell Sci.* **122,** 893–903
15. Chhabra, E. S., and Higgs, H. N. (2007) The many faces of actin: matching assembly factors with cellular structures. *Nat. Cell Biol.* **9,** 1110–1121
16. Burgoyne, R. D., and Morgan, A. (2003) Secretory granule exocytosis. *Physiol. Rev.* **83,** 581–632
17. Sokac, A. M., and Bement, W. M. (2006) Kiss-and-coat and compartment mixing: coupling exocytosis to signal generation and local actin assembly. *Mol. Biol. Cell* **17,** 1495–1502
18. Orci, L., Gabbay, K. H., and Malaisse, W. J. (1972) Pancreatic β-cell web: its possible role in insulin secretion. *Science* **175,** 1128–1130
19. Somers, G., Blondel, B., Orci, L., and Malaisse, W. J. (1979) Motile events in pancreatic endocrine cells. *Endocrinology* **104,** 255–264
20. Snabes, M. C., and Boyd, A. E., 3rd (1982) Increased filamentous actin in islets of Langerhans from fasted hamsters. *Biochem. Biophys. Res. Commun.* **104,** 207–211
21. Howell, S. L., and Tyhurst, M. (1986) The cytoskeleton and insulin secretion. *Diabetes Metab. Rev.* **2,** 107–123
22. Li, G., Rungger-Brändle, E., Just, I., Jonas, J. C., Aktories, K., and Wollheim, C. B. (1994) Effect of disruption of actin filaments by *Clostridium botulinum* C2 toxin on insulin secretion in HIT-T15 cells and pancreatic islets. *Mol. Biol. Cell* **5,** 1199–1213
23. Mourad, N. I., Nenquin, M., and Henquin, J. C. (2010) Metabolic amplifying pathway increases both phases of insulin secretion independently of β-cell actin microfilaments. *Am. J. Physiol. Cell Physiol.* **299,** C389–C398
24. Hammar, E., Tomas, A., Bosco, D., and Halban, P. A. (2009) Role of the Rho-ROCK (Rho-associated kinase) signaling pathway in the regulation of pancreatic β-cell function. *Endocrinology* **150,** 2072–2079
25. Nevins, A. K., and Thurmond, D. C. (2003) Glucose regulates the cortical actin network through modulation of Cdc42 cycling to stimulate insulin secretion. *Am. J. Physiol. Cell Physiol.* **285,** C698–C710
26. Kowluru, A., and Veluthakal, R. (2005) Rho guanosine diphosphate-dissociation inhibitor plays a negative modulatory role in glucose-stimulated insulin secretion. *Diabetes* **54,** 3523–3529
27. Lopez, J. P., Turner, J. R., and Philipson, L. H. (2010) Glucose-induced ERM protein activation and translocation regulates insulin secretion. *Am. J. Physiol. Endocrinol. Metab.* **299,** E772–E785
28. Kepner, E. M., Yoder, S. M., Oh, E., Kalwat, M. A., Wang, Z., Quilliam, L. A., and Thurmond, D. C. (2011) Cool-1/ βPIX functions as a guanine nucleotide exchange factor in the cycling of Cdc42 to regulate insulin secretion. *Am. J. Physiol. Endocrinol. Metab.* **301,** E1072–E1080
29. Etienne-Manneville, S. (2004) Cdc42–the centre of polarity. *J. Cell Sci.* **117,** 1291–1300
30. Takenawa, T., and Suetsugu, S. (2007) The WASP-WAVE protein network: connecting the membrane to the cytoskeleton. *Nat. Rev. Mol. Cell Biol.* **8,** 37–48
31. Garvalov, B. K., Flynn, K. C., Neukirchen, D., Meyn, L., Teusch, N., Wu, X., Brakebusch, C., Bamburg, J. R., and Bradke, F. (2007) Cdc42 regulates cofilin during the establishment of neuronal polarity. *J. Neurosci.* **27,** 13117–13129
32. Sumi, T., Matsumoto, K., Takai, Y., and Nakamura, T. (1999) Cofilin phosphorylation and actin cytoskeletal dynamics regulated by rho- and Cdc42-activated LIM-kinase 2. *J. Cell Biol.* **147,** 1519–1532
33. Condeelis, J. (2001) How is actin polymerization nucleated *in vivo*? *Trends Cell Biol.* **11,** 288–293
34. Carlier, M. F., Ressad, F., and Pantaloni, D. (1999) Control of actin dynamics in cell motility. Role of ADF/cofilin. *J. Biol. Chem.* **274,** 33827–33830
35. Oser, M., Yamaguchi, H., Mader, C. C., Bravo-Cordero, J. J., Arias, M., Chen, X., Desmarais, V., van Rheenen, J., Koleske, A. J., and Condeelis, J. (2009) Cortactin regulates cofilin and N-WASp activities to control the stages of invadopodium assembly and maturation. *J. Cell Biol.* **186,** 571–587
36. Gong, C., Stoletov, K. V., and Terman, B. I. (2004) VEGF treatment induces signaling pathways that regulate both actin polymerization and depolymerization. *Angiogenesis* **7,** 313–321
37. Iwasaki, M., Minami, K., Shibasaki, T., Miki, T., Miyazaki, J., and Seino, S. (2010) Establishment of new clonal pancreatic β-cell lines (MIN6-K) useful for study of incretin/cyclic adenosine monophosphate signaling. *J. Diabetes Invest.* **1,** 137–142
38. Moriyama, K., Iida, K., and Yahara, I. (1996) Phosphorylation of Ser-3 of cofilin regulates its essential function on actin. *Genes Cells* **1,** 73–86
39. Miki, H., Miura, K., and Takenawa, T. (1996) N-WASP, a novel actin-depolymerizing protein, regulates the cortical cytoskeletal rearrangement in a PIP2-dependent manner downstream of tyrosine kinases. *EMBO J.* **15,** 5326–5335
40. Kashima, Y., Miki, T., Shibasaki, T., Ozaki, N., Miyazaki, M., Yano, H., and Seino, S. (2001) Critical role of cAMP-GEFII-Rim2 complex in incretin-potentiated insulin secretion. *J. Biol. Chem.* **276,** 46046–46053
41. Yasuda, T., Shibasaki, T., Minami, K., Takahashi, H., Mizoguchi, A., Uriu, Y., Numata, T., Mori, Y., Miyazaki, J., Miki, T., and Seino, S. (2010) Rim2α determines docking and priming states in insulin granule exocytosis. *Cell Metab.* **12,** 117–129
42. Sugawara, K., Shibasaki, T., Mizoguchi, A., Saito, T., and Seino, S. (2009) Rab11 and its effector Rip11 participate in regulation of insulin granule exocytosis. *Genes Cells* **14,** 445–456

43. Ridley, A. J. (2006) Rho GTPases and actin dynamics in membrane protrusions and vesicle trafficking. *Trends Cell Biol.* **16,** 522–529
44. Dovas, A., and Cox, D. (2010) Regulation of WASP by phosphorylation: Activation or other functions? *Commun. Integr. Biol.* **3,** 101–105
45. Thurmond, D. C., Gonelle-Gispert, C., Furukawa, M., Halban, P. A., and Pessin, J. E. (2003) Glucose-stimulated insulin secretion is coupled to the interaction of actin with the t-SNARE (target membrane soluble *N*-ethylmaleimide-sensitive factor attachment protein receptor protein) complex. *Mol. Endocrinol.* **17,** 732–742
46. Bernard, O. (2007) Lim kinases, regulators of actin dynamics. *Int. J. Biochem. Cell Biol.* **39,** 1071–1076
47. Bernstein, B. W., and Bamburg, J. R. (2010) ADF/cofilin: a functional node in cell biology. *Trends Cell Biol.* **20,** 187–195
48. DesMarais, V., Ghosh, M., Eddy, R., and Condeelis, J. (2005) Cofilin takes the lead. *J. Cell Sci.* **118,** 19–26
49. Sumi, T., Matsumoto, K., and Nakamura, T. (2001) Specific activation of LIM kinase 2 via phosphorylation of threonine 505 by ROCK, a Rho-dependent protein kinase. *J. Biol. Chem.* **276,** 670–676
50. Shi, Y., Pontrello, C. G., DeFea, K. A., Reichardt, L. F., and Ethell, I. M. (2009) Focal adhesion kinase acts downstream of EphB receptors to maintain mature dendritic spines by regulating cofilin activity. *J. Neurosci.* **29,** 8129–8142
51. Smythe, E., and Ayscough, K. R. (2006) Actin regulation in endocytosis. *J. Cell Sci.* **119,** 4589–4598
52. Malacombe, M., Bader, M. F., and Gasman, S. (2006) Exocytosis in neuroendocrine cells: new tasks for actin. *Biochim. Biophys. Acta* **1763,** 1175–1183
53. Lopez, J. A., Burchfield, J. G., Blair, D. H., Mele, K., Ng, Y., Vallotton, P., James, D. E., and Hughes, W. E. (2009) Identification of a distal GLUT4 trafficking event controlled by actin polymerization. *Mol. Biol. Cell* **20,** 3918–3929
54. Gasman, S., Chasserot-Golaz, S., Malacombe, M., Way, M., and Bader, M. F. (2004) Regulated exocytosis in neuroendocrine cells: a role for subplasmalemmal Cdc42/N-WASP-induced actin filaments. *Mol. Biol. Cell* **15,** 520–531
55. Suetsugu, S., Hattori, M., Miki, H., Tezuka, T., Yamamoto, T., Mikoshiba, K., and Takenawa, T. (2002) Sustained activation of N-WASP through phosphorylation is essential for neurite extension. *Dev. Cell* **3,** 645–658
56. Morreale, A., Venkatesan, M., Mott, H. R., Owen, D., Nietlispach, D., Lowe, P. N., and Laue, E. D. (2000) Structure of Cdc42 bound to the GTPase binding domain of PAK. *Nat. Struct. Biol.* **7,** 384–388
57. van Obberghen, E., Somers, G., Devis, G., Vaughan, G. D., Malaisse-Lagae, F., Orci, L., and Malaisse, W. J. (1973) Dynamics of insulin release and microtubular-microfilamentous system. I. Effect of cytochalasin B. *J. Clin. Invest.* **52,** 1041–1051
58. Wang, Z., Oh, E., Clapp, D. W., Chernoff, J., and Thurmond, D. C. (2011) Inhibition or ablation of p21-activated kinase (PAK1) disrupts glucose homeostatic mechanisms *in vivo*. *J. Biol. Chem.* **286,** 41359–41367
59. Cerasi, E., and Luft, R. (1967) The plasma insulin response to glucose infusion in healthy subjects and in diabetes mellitus. *Acta Endocrinol.* **55,** 278–304
60. Davis, S. N., Piatti, P. M., Monti, L., Brown, M. D., Branch, W., Hales, C. N., and Alberti, K. G. (1993) Proinsulin and insulin concentrations following intravenous glucose challenges in normal, obese, and non-insulin-dependent diabetic subjects. *Metabolism* **42,** 30–35